

Lab on a Chip

Accepted Manuscript



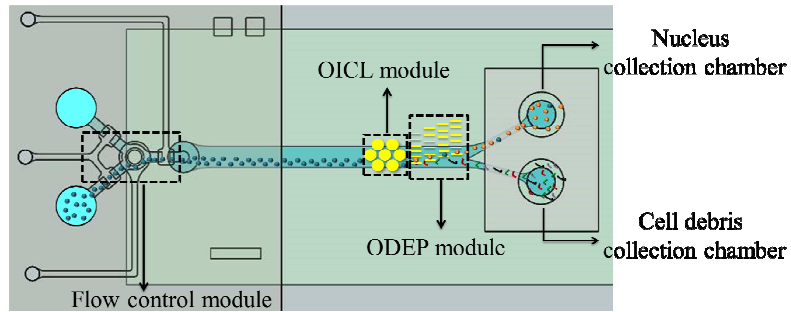
This is an *Accepted Manuscript*, which has been through the Royal Society of Chemistry peer review process and has been accepted for publication.

Accepted Manuscripts are published online shortly after acceptance, before technical editing, formatting and proof reading. Using this free service, authors can make their results available to the community, in citable form, before we publish the edited article. We will replace this *Accepted Manuscript* with the edited and formatted *Advance Article* as soon as it is available.

You can find more information about *Accepted Manuscripts* in the [Information for Authors](#).

Please note that technical editing may introduce minor changes to the text and/or graphics, which may alter content. The journal's standard [Terms & Conditions](#) and the [Ethical guidelines](#) still apply. In no event shall the Royal Society of Chemistry be held responsible for any errors or omissions in this *Accepted Manuscript* or any consequences arising from the use of any information it contains.

An innovative, microfluidics-based approach featuring optically-induced cell lysis (OICL) for nucleus extraction and collection in an automatic format was demonstrated. The efficiency of cell membrane lysis and the ODEP nucleus separation were measured to be $78.04 \pm 5.70\%$ and $80.90 \pm 5.98\%$, respectively, leading to an overall nucleus extraction efficiency of $58.21 \pm 2.21\%$.



ARTICLE

Continuous Nucleus Extraction by Optically-Induced Cell Lysis on a Batch-type Microfluidic Platform[†]

Cite this: DOI: 10.1039/x0xx00000x

Shih-Hsuan Huang^a, Lien-Yu Hung^a and Gwo-Bin Lee^{a, b, c*}Received 00th October 2015,
Accepted 00th December 2015

DOI: 10.1039/x0xx00000x

www.rsc.org/

The extraction of a cell's nucleus is an essential technique required for a number of procedures, such as disease diagnosis, genetic replication, and animal cloning. However, existing nucleus extraction techniques are relatively inefficient and labor-intensive. Therefore, this study presents an innovative, microfluidics-based approach featuring optically-induced cell lysis (OICL) for nucleus extraction and collection in an automatic format. In comparison to previous micro-devices designed for nucleus extraction, the new OICL device designed herein is superior in terms of flexibility, selectivity, and efficiency. To facilitate this OICL module for continuous nucleus extraction, we further integrated an optically-induced dielectrophoresis (ODEP) module with the OICL device within the microfluidic chip. This on-chip integration circumvents the need for highly trained personnel and expensive, cumbersome equipment. Specifically, this microfluidic system automates four steps by 1) automatically focusing and transporting cells, 2) releasing the nuclei on the OICL module, 3) isolating the nuclei on the ODEP module, and 4) collecting the nuclei in the outlet chamber. The efficiency of cell membrane lysis and the ODEP nucleus separation were measured to be $78.04 \pm 5.70\%$ and $80.90 \pm 5.98\%$, respectively, leading to an overall nucleus extraction efficiency of $58.21 \pm 2.21\%$. These results demonstrate that this microfluidics-based system can successfully perform nucleus extraction, and the integrated platform is therefore promising in cell fusion technology with the goal of achieving genetic replication, or even animal cloning, in the near future.

Introduction

Nucleus extraction has been widely utilized in various biological applications, including disease detection [1], molecular cytogenetic investigations [2], enzyme studies [3] and even nuclear transfer procedures [4]. In eukaryotes, nuclei typically house nearly all of cell's genetic materials, which are organized as multiple chromosomes. Therefore, a variety of molecular and cell biology protocols depend upon cell lysis and consequent collection of the targeted cellular material(s)/macromolecules [5], indicating that nucleus extraction is a crucial process. However, most of existing protocols for nucleus extraction rely on cell lysis/membrane disruption to release the nuclei, as well as other cellular constituents, into the media [6, 7], which may require subsequent tedious purification process.

Cell lysis can be accomplished by thermal, electrical, chemical, acoustical, optical, or mechanical methods [8]. Conventionally, cells have commonly been lysed by chemical and mechanical (e.g., homogenizing) methods. As the cell membrane consists of a lipid bilayer, lysis buffers containing surfactants allow for the solubilisation of the lipid membrane and subsequent release of all intracellular materials. In many of these processes, the organelle membranes are also dissolved by these buffers, thereby making it difficult to determine the organelle/protein of origin. In the case of mechanical lysis, a similar issue prevails; not only is structural information lost (e.g., the cellular location of an organelle or macromolecule), but most intracellular components are damaged [9, 10].

Alternatively, thermal lysis is commonly used to isolate nucleic acids. At high temperatures, proteins within the cell membranes denature irreparably, damaging the cell and releasing the intracellular substances. However, this method is only compatible with nucleic acid analysis as the proteins are typically irreversibly denatured during the course of the heating [11]. Recently, electrical [10] and acoustic devices [12, 13] have been developed for cell lysis. The former relies on using relatively high electrical fields to disrupt cell membranes. Nevertheless, conventional electrical methods based on microelectrodes are usually limited by the electrodes' position because only cells near the electrodes could be lysed. Additionally, application of high voltage is necessary to induce efficient cell lysis, which in turn leads to heat generation that could cause adverse effects such as organelle damage [10]. Alternatively, when using acoustic approaches, heat generation by absorption of acoustic energy at durations over 50 seconds could also damage intracellular macromolecules and, notably, denature proteins accordingly [12, 13].

To overcome some of the difficulties associated with cell membrane lysis and nucleus extraction mentioned above, microfluidic technologies have been demonstrated recently. For instance, a method featuring a magnetically-driven microtool (MMT) was robotically controlled in a microfluidic chip by using permanent magnets and used for nucleus isolation [14, 15]. Similarly, a robotic, microfluidic device for extraction of nuclei from oocytes was reported [16]. However, the yield of viable nuclei was relatively low, and the operation time was lengthy [16].

Recently, an optically-induced cell lysis (OICL) device which could selectively disrupt the cell membrane without damaging the nucleus by adjusting the power density of the illumination light spot was reported by our group [17]. The OICL device consisted of an

indium-tin-oxide (ITO)-coated glass and a photoconductive layer (hydrogenated amorphous silicon, a-Si: H) [18]. Different light patterns can be programmed and then projected to serve as “virtual” electrodes on a microfluidic platform via a digital projector. In comparison to fixed-electrode based devices, this device can generate locally enhanced electrical fields, and is highly flexible and selective since only cells under light illumination could be lysed. Notably, it can selectively disrupt cell membranes without damaging the nucleus, thus making it amenable to nucleus extraction procedures. Furthermore, when compared with conventional electric approaches, less heat is generated when optically lysing cells [8]. Furthermore, this approach is relatively simple and requires no lithographic process to fabricate microelectrodes [17]. This OICL chip, therefore, has provided a convenient, simple, and powerful means of extracting cell nuclei. However, the throughput of the microfluidic device still remains an issue.

ODEP (optically-induced dielectrophoresis), or “optical tweezers,” has been demonstrated as a powerful tool for manipulation of microparticles or cells [18]. Briefly, when pre-programmed light is projected onto the a-Si: H layer and an alternating current is applied onto the top and bottom ITO layers of the ODEP device, a “virtual” electrode is formed that generates a non-uniform electrical field to induce dielectrophoretic (DEP) force. Upon integration of an ODEP system into a microfluidic chip, a group of cells or differently sized particles could be separated [18, 19-20]. In this work, we therefore demonstrate a new microfluidic device, which not only conducts OICL for selective cell membrane lysis, but also execute ODEP-based separation for nucleus collection. Herein OICL and ODEP were integrated into a single microfluidic system to serve as a streamlined means to 1) lyse cell membranes without disrupting their nuclei and 2) separate intact nuclei from cellular membrane debris. This is the first time that an integrated microfluidic device has been demonstrated to extract and collect nuclei in a continuous-flow platform. Given these attributes, this integrated microfluidic chip could be widely applicable in future nuclear transfer applications and particularly for genetic replication and animal cloning studies.

Materials and methods

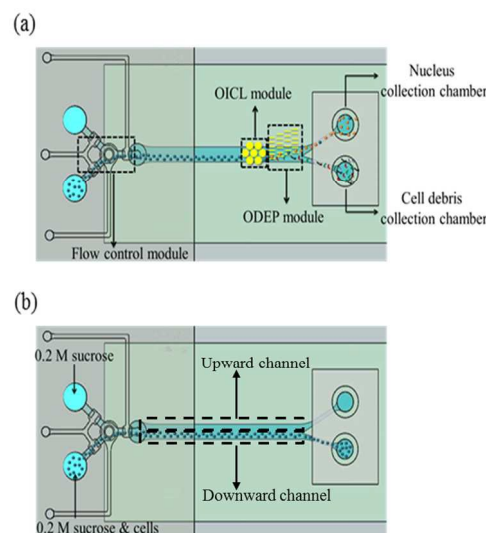
Experimental procedure

The experimental process for the integrated OICL/ODEP chip for continuous nucleus extraction is schematically illustrated in Fig. 1(a). In order to perform nucleus extraction in an automated manner, we integrated three modules on a single chip, including a flow control module, an OICL module and an ODEP module. The flow control module was composed a suction-type, pneumatic micropump [21] to transport cells, normally-closed microvalves to control fluid flow, microchannels and inlet/outlet chambers. The OICL module was used to generate an optically-induced, non-uniform electrical field for selectively disrupting cell membrane to release the nucleus. The ODEP module used moving light-bars for separation of cell debris such that nuclei could be collected in the outlet chamber.

The experimental procedures for continuous nucleus extraction on the integrated microfluidic chip could be described as follows. HEK293T cells (human embryonic kidney cell, ATCC® CRL-11268TM, USA) were first suspended in 0.2 M sucrose buffer (“sample flow”). Note that the concentration of HEK293T cell suspension was 10^4 cells/ml. Two inlet chambers (for injecting 0.2 M sucrose and HEK293T cells suspended in 0.2 M sucrose) equipped with a

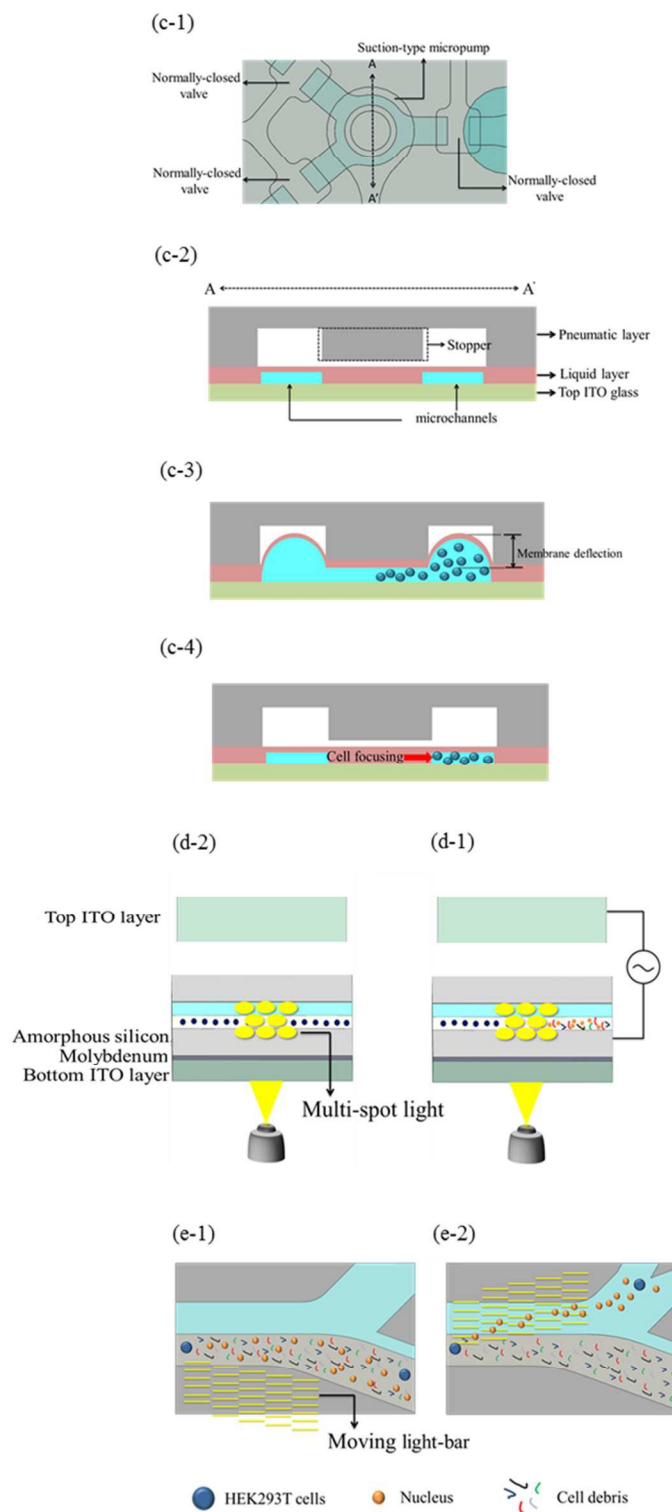
suction-type micropump were designed to hydrodynamically focus cells into the downward channel. Note that cells were transported by the suction-type micropump and hydrodynamically focused in the downward channel while another 0.2 M sucrose buffer flow was simultaneously transported (Fig. 1(b)). The detail information about the suction-type micropump could be found in our previous work [21]. Briefly, the deflection of the PDMS membrane produced a suction force to achieve the fluid flow such that hydrodynamic focusing of cells could be achieved, as schematically illustrated in Fig. 1(c). Note that the hydrodynamic focusing of the cells to the downward region of the channel plays an important role for the yield of cell debris separation. For achieving cell membrane lysis by OICL followed by cell debris separation by ODEP, we controlled the transport volume rate of the suction-type micropump with a polydimethylsiloxane (PDMS) cylinder as a stopper (Fig. 1(c-2)), which was located on the pneumatic layer to precisely control the deflection of the PDMS membrane [22], such that an exact amount of sample could be transported to the subsequent OICL and ODEP zones of the chip.

Cell membrane lysis was conducted in the OICL module and cell debris and nuclei were separated by the force generated by the ODEP module. Note that the chip was operated in a batch-type manner, with defined volumes of cell suspension being delivered in cycles. We designed a suction-type micropump to serve as the flow control module to transport a fixed amount of cell samples from the OICL module to the ODEP module. In the cell lysis zone, as shown in Fig 1(d), multiple light spots (diameter of each spot = 75 μm) were projected from a digital projector, and a non-uniform electrical field was generated accordingly to create a required transmembrane potential across the cell membrane if the top and bottom ITO glass substrate were applied with an alternating-current (AC) voltage. In this study, we used the multi-spot light as virtual electrodes to improve the lysis efficacy since it may generate more locally-enhanced electric field such that all cells membrane in this zone could be disrupted without damaging the nuclei. The light intensity of the virtual electrodes was 3.2 W/cm^2 (white light), which allowed the HEK293T cell membranes to be lysed without disruption of the nuclei. After cell membrane lysis, cell debris, nuclei, and non-lysed cells passed through the moving light-bar zone of the ODEP module. The moving light-bar zone (each light-bar length (L) = 211.3 μm , width (W) = 15.8 μm) contained three



sections, which could drag cells/nuclei/debris upwards by ODEP force. The maximum dragging velocity varied for nuclei, non-lysed cells and cell debris and therefore the nuclei were separated and then collected in the upper chamber (nucleus extraction chamber) (Fig. 1e).

Figure 1: (a) Schematic illustration of the experimental procedure performed on an integrated OICL/ODEP chip. (b) The flow control module was used for guiding cells in the downward channel. (c) Schematic illustration of the focusing mechanism used to guide cells. (c-1 - c-2) The PDMS membrane produces a suction force to control both the 0.2 M sucrose solution alone and the HEK293T cells suspended in 0.2 M sucrose within the transport unit (micropump). (c-2 - c-3) When transporting samples into the downward channel, the PDMS membrane generates sufficient pressure to push HEK293T cells in 0.2 M sucrose into the downward channel, while simultaneously focusing them. (d) Cell membranes were lysed as they passed through the OICL module. (e) In the ODEP module, the nuclei, non-lysed cells and debris were sorted by size, as differently sized particles induce differing ODEP forces.



Chip design and fabrication

In order to rapidly transport, focus, and lyse cell membranes, a flow control module for fluid transport/focus, an OICL module for cell membrane lysis and an ODEP module for nucleus collection were integrated on a single microfluidic chip (Fig. 2). A layer-by-layer view of the fabricated chip is shown in Fig. 2(a). This chip consisted of a suction-type micropump on the top substrate and an OICL module and an ODEP module on the bottom substrate. Specifically, the flow control module contained a pneumatic micropump with a PDMS cylinder as a stopper, three normally-closed microvalves, inlet and outlet chambers, and microchannels; all microfluidic components were fabricated by using a PDMS replication process. The microstructure was consisted of polyethymethacrylate (PMMA) molds that were shaped by a computer-numerical-control (CNC) machine (EGC-400, Roland Inc., Japan) equipped with a 0.5- mm drill bit [21]. Then, all of the microstructures were replicated by a PDMS (Sylgard 184A/B, Dow Corning Corp, USA) soft lithography technique from the PMMA molds [21]. The chip consisted of five layers, including a pneumatic layer, a liquid layer, an ITO glass layer, a 30- μm thick layer of double-sided tape, and another bottom ITO glass layer surface-coated with a-Si:H. The thickness of the pneumatic layer was 1 cm. The thickness of the liquid layer was 200 μm , and the PDMS membrane of the micropumps and microvalves was only 100 μm . Finally, the two PDMS structures (including a pneumatic layer and a liquid layer) and the ITO glass layer were bonded together by an oxygen plasma treatment. After guiding the flow control module on the top ITO, another bottom ITO glass surface-coated with an a-Si:H layer was assembled while a 30- μm double-sided tape with laser-machined Y-shaped channel was used for packaging. Note that the bottom ITO glass was consisted of an ITO glass, a 10-nm-thick molybdenum metal layer, and a 1- μm -thick a-Si:H coating, which served as a photoconductive layer for generating optically-induced cell membrane lysis and optically-induced nucleus extraction. Note that the double-sided tape was used as an adhesive layer between the top ITO glass and the bottom ITO glass. Furthermore, microchannels were formed with a CO₂ laser cutter (VL-200, Universal Laser Systems, Scottsdale, USA). A photograph of the assemble chip is shown in Fig. 2(b) with dimensions of 35 mm x 45 mm. The detailed layout of the microfluidic platform, including the flow control module, the OICL module, and the ODEP module, has been shown in Figs. 2(c) and 2(d).

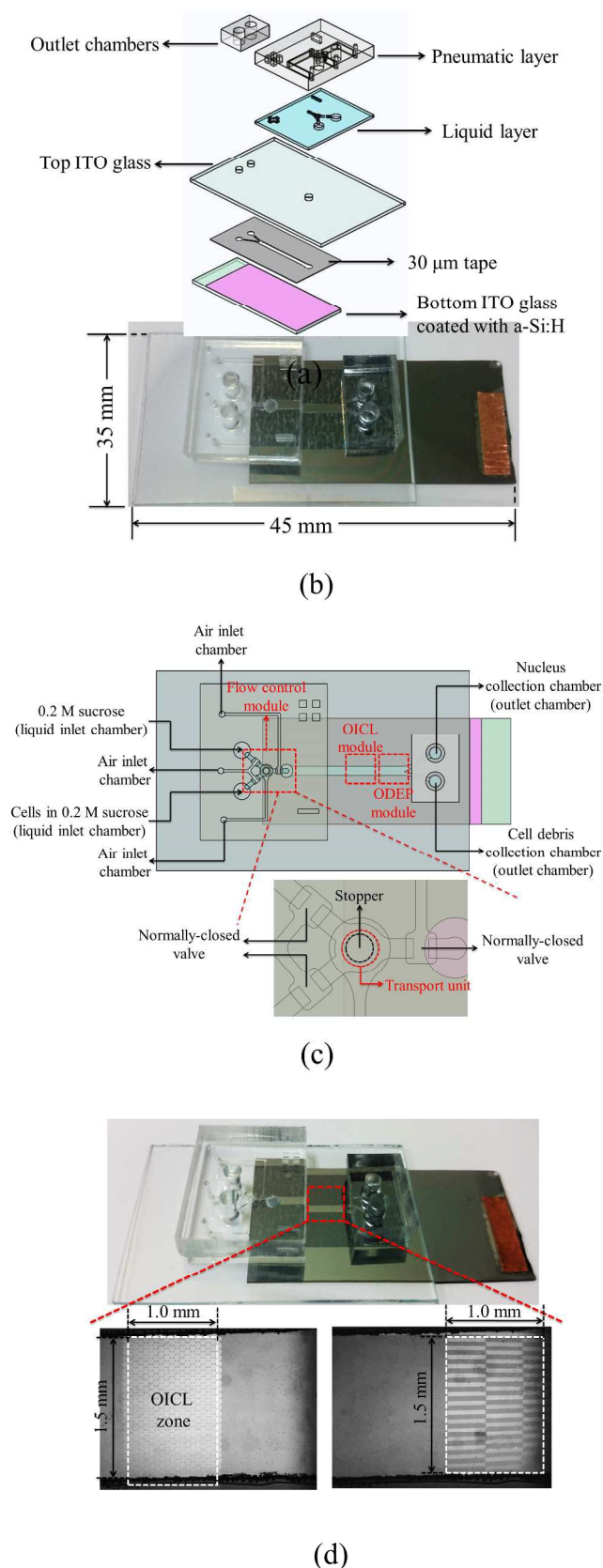


Figure 2. (a) An exposed view of the integrated OICL/ODEP chip consisted of (from top to bottom) a pneumatic layer, a liquid layer, a top ITO layer, a 30- μm thick layer of double-sided tape, and another

bottom ITO glass layer surface-coated with *a-Si:H*. (b) A photograph of assembled OICL/ODEP chip (35 mm x 45 mm). (c) Flow control, OICL, and ODEP modules were integrated into a microfluidic platform for continuous nucleus extraction. The former consisted of three normally-closed valves, a micropump, inlet/outlet chambers and microchannels. When injected with 0.2 M sucrose and cells suspended in 0.2 M sucrose, the flow control module transports a group of cells into the OICL and ODEP modules for nucleus extraction. (d) The location of the OICL and ODEP zones in the integrated OICL/ODEP chip, as well as pictures of these modules. Note that "arrayed spot-" and "moving bar-" patterned light was irradiated onto the microchannel by a digital projector. The dimensions of the OICL and ODEP zones were 1.5 cm x 1.0 cm.

Focusing and pumping devices in the flow control module

In order to transport an exact volume of cell samples from the cell membrane lysis zone (i.e., OICL module) to the moving light-bar zone (i.e., ODEP module), 0.2 M sucrose alone and HEK293T cells suspended in 0.2 M sucrose were injected into the corresponding inlet chambers to guide in the flow control module (Fig. 2c), which was composed of a pneumatically-driven micropump and three microvalves [21]. Then, the PDMS membrane above the liquid layer was deflected upwards to create a vacuum (i.e., negative air gauge pressure). The difference in pressure allowed the re-suspended HEK293T cells (in 0.2 M sucrose buffer) to be transported to the OICL module and, later, the ODEP separation zone. Moreover, a cylindrical PDMS plug was designed into the middle of the microchamber in the pneumatic layer and acted as a stopper (Fig. 1(c-2)). When different negative gauge pressures were applied upon the pneumatic layer, the PDMS membrane in the liquid channel was deflected upwards and stopped by coming into contact with the PDMS plug, which could, in turn, control and regulate the consistency of the transported volume [22] into the OICL and ODEP manipulation zones. Note that precise control of the cell samples in these two zones is crucial since we would like to assure most cells membranes have been lysed and sorted. In addition, the PDMS membrane could produce suction forces to control the flow of 0.2 M sucrose and HEK293T cells suspended in 0.2 M sucrose throughout the transport unit (micropump) precisely. The PDMS membrane could also generate sufficient pressure (force) to push cells into the downward channel during the cell focusing process. Therefore, the cells could be successfully guided and transported into OICL/ODEP zone for separating nuclei into the outlet chamber.

Cell membrane lysis in the OICL module

In this study, virtual electrodes were used to produce a sufficient enough transmembrane potential across the cell membrane to cause cell membrane lysis without disruption of the nucleus [17]. The OICL device developed herein consisted of two ITO glass layers and a double-side tape equipped with a Y-shaped channel (Fig. 2(a)). Furthermore, the bottom ITO glass was coated with a photoconductive layer (*a-Si:H*). An AC voltage was first applied between the two ITO layers. In the absence of light, no DEP force was generated. However, upon light illumination, the resistance of the photo-conductive layer (in the illuminated zones) was decreased by more than 4-5 orders of magnitude [17, 23] due to the creation of electron-hole pairs. This phenomenon caused a strong, non-uniform electrical field to be generated in the liquid layer. A transmembrane potential ($\Delta\phi$) is then induced. If the transmembrane potential exceeds a critical threshold value, the cell's membrane is permeabilized, allowing exogenous molecules (ex. plasmid DNA) to enter the cell. When the transmembrane potential is higher than ~ 1

V, irreversible electroporation of the cell membrane followed by lysis occurs [17].

The transmembrane potential of a cell under an AC electrical field is typically modelled by the Schwan equation [24].

$$\Delta\psi_{membr} = \frac{1.5 a E_{appl} \cos \theta}{(1 + (\omega_{ac}\tau)^2)^{1/2}}$$

where $\tau = aC_{membr}(\rho_{int} + \rho_{ext}/2)$. The terms of a , E_{appl} , and θ are the outer cell radius, the applied electrical field, and the angle between the field line and perpendicular (normal) to the point of interest, respectively. Furthermore, ω_{ac} , C_{membr} , ρ_{int} and ρ_{ext} are the angular frequency of the applied electric field, the capacitance of the membrane, the resistivity of the internal medium, and the resistivity of the external medium, respectively. In order to only lyse cell membranes, not nuclear envelopes, the applied AC voltage was optimized to be 24 volts at a frequency of 8.5 kHz [8]. The transmembrane potential of a cell under the applied AC electrical field was calculated in Supplemental Table S1 and Supplemental Figure S2.

Nuclei collection in the ODEP module

As mentioned previously, when light irradiation and an AC voltage are applied onto the ITO layers, a non-uniform electrical field is induced locally and accordingly an ODEP force could be generated for the manipulation of nucleus and cells. When the cells passed through the cell membrane lysis zone, most of the cell membranes were lysed and nuclei were released, and the ODEP force produced acted to separate the nuclei from the cell debris because different sizes of particles experienced different ODEP force. From the time-averaged ODEP force equation ($F(t) = 2\pi r^3 \epsilon_m^* (Re f_{CM}) \nabla E^2$, where r = radius of microparticles) [25], when the optically-induced moving-bars (dimensions of the moving-bars: width = 60 μm and length = 400 μm) were generated and projected on the ODEP separation zone, the nuclei (size: 3-5 μm) and cell debris (size: <1 μm) experienced different positive ODEP forces. The ODEP force exerted on nuclei was much stronger than cell debris (up to 1-2 orders of magnitude) so that the nuclei were separated from cell debris. Finally, the extracted nuclei were collected from the outlet chamber of the microfluidic chip. The calculation of the ODEP drag forces could be found in Supplemental Information and our previous work [28].

Sample preparation

HEK293T cell lines (human embryonic kidney cell, ATCC® CRL-11268TM, USA) were cultured in Dulbecco's Modified Eagle Medium (DMEM; 10 ml, Life Technologies, USA) with 10% fetal bovine serum (FBS, 1 ml, Life Technologies). They were trypsinized (1% in phosphate buffered saline (PBS), 1 ml, Biowest Inc., France) and suspended in 3 ml of DMEM. The cells were washed and re-suspended in PBS (1x, 2 ml, Biowest Inc., France) at a final concentration of 5×10^6 cells/ml in 2 ml. For nucleus and membrane staining, 2 μl of SYTO® 14 Green Fluorescent Nucleic Acid Stain (Molecular Probes, USA) and 2 μl of CellMask Deep Red plasma membrane stain (Molecular Probes, USA) were added to 2 ml of cell suspension (concentration = 5×10^6 cells/ml) and incubated for 20 min. PBS buffer was then replaced with 2 ml of 0.2 M sucrose buffer twice for subsequent use in cell membrane lysis and ODEP separation experiments. The final concentration of the HEK293T cell suspension (OICL/ODEP sample) was 10^4 cells/ml.

Experimental setup

The experimental setup has been illustrated in Fig. 3. Samples were first loaded into the inlet chamber, and the cell sample was then transported and focused by then pneumatic micropump. It was also comprised of a personal computer, 10 electromagnetic valves (EMVs, SD70M-6BG, SMC Inc., Japan), an air compressor (MDR2-1A/11, Jun-Air Inc., Japan), and a vacuum pump (DF-506, DFMI co., Ltd, Taiwan). The HEK293T cells were focused/guided and transported into the OICL/ODEP zones. A digital projector (PLC-XU106, SANYO, USA) was used to generate optical patterns programmed with Adobe Flash (Adobe Systems Inc., USA) to serve as virtual electrodes on the OICL/ODEP modules. Two 20x objective lenses (Nikon, Japan) were positioned between the projector and the OICL/ODEP chip to focus the programmed light patterns on the OICL/ODEP chip. An image acquisition system (Evolution VF, Media Cybernetics, Inc., USA) consisting of a charge-coupled device (CCD) camera (Evolution VF, Nikon, Canada) and an optical microscope (BX43, Olympus, Japan) were placed on top of the OICL/ODEP chip to observe cell membrane lysis and nucleus collection. An AC voltage was generated by a function generator (AFG-2125, Good Will Instrument Co., Ltd., Taiwan) and amplified by a power amplifier (HA-405, PINTEK, Taiwan) to lyse the cell membrane and to separate the nucleus from cellular debris. The output voltage was monitored by a digital oscilloscope (GDS-1102-U, Good Will Instrument Co., Ltd., Taiwan). Note that the frequency and magnitude of the AC voltage was administered in a fashion that would generate a non-uniform electrical field across the top and bottom ITO layers of the OICL/ODEP chip to achieve cell membrane lysis and subsequent nuclear extraction. Furthermore, the fluorescence staining samples were then observed and counted by using a fluorescent microscope containing one collimation lens, one objective lens (Nikon LU Plan 10x/0.30 A, Nikon, Japan), one mercury lamp (MODEL C-SHG1, Nikon, Japan), and three fluorescence filters (Nikon G-2A, Nikon, Japan). Images were captured using a CCD camera coupled to an inverted microscope equipped with a digital control module. Counted image data were measured from three repeated experiments and further analyzed to calculate the mean value and the standard deviation [27, 28].

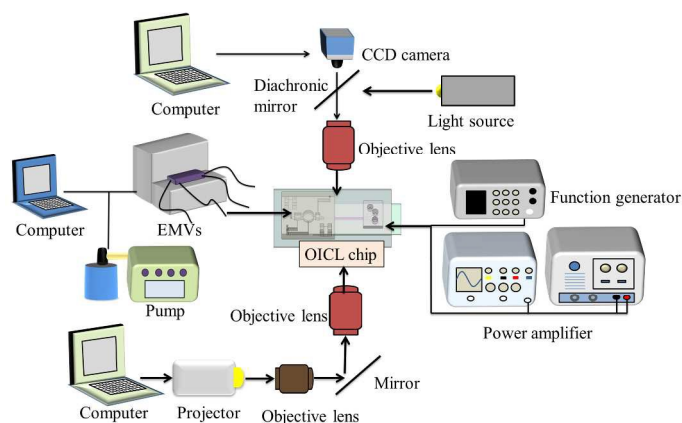


Figure 3: Experimental setup for extraction of nuclei from cells by OICL and ODEP on a continuous microfluidic platform. Cells in 0.2 M sucrose were injected by a suction-type micropump and allowed to flow through the OICL and ODEP modules. The cells were lysed, and cell debris was separated

from the extracted nuclei, which were then collected from the outlet chambers.

Evaluation of the cell membrane lysis rate, the ODEP nucleus separation rate, and the overall nucleus extraction rate

For visualization of cell membrane lysis using OICL without disruption of the nucleus, we utilized a dual-staining approach to observe the fate of the cell membranes and nuclei in real time. The fluorescent dye, CellMask Deep Red (Molecular Probes, USA) provides excellent and rapid plasma membrane staining in live cells, and therefore was used to stain cell membrane in this study [26]. HEK293T were incubated with 1 $\mu\text{g}/\text{mL}$ CellMask Deep Red plasma membrane stain at 37°C for 20 minutes and pelleted again at 100000 g to remove any excessive dye. Another fluorescent dye, SYTO[®] 14 Green (Molecular Probes, USA) was used to stain the nucleus [27]. HEK293T were incubated with 0.9 $\mu\text{g}/\text{mL}$ SYTO[®] 14 Green stain at 37°C for 20 minutes and pelleted again at 100000 g to remove any excessive dye. After choosing suitable fluorescence stains, the cell membrane lysis rate, nucleus separation rate, and overall nucleus extraction rate could be calculated as follows.

Cell membrane lysis rate (%)

$$= \frac{\text{Cells only expressing green fluorescence}}{\text{Total number of cells}} \times 100\%$$

Nucleus separation rate (%)

$$= \frac{\text{Cells only expressing green fluorescent in upward channel}}{\text{Total number of cells only expressing green fluorescence}} \times 100\%$$

Overall nucleus extraction rate (%)

$$= \frac{\text{Number of cells expressing green fluorescence in upward channel}}{\text{Total number of cells}} \times 100\%$$

Note that the overall nucleus extraction rate was the product of the cell membrane lysis rate and the nucleus separation rate.

Results and discussion

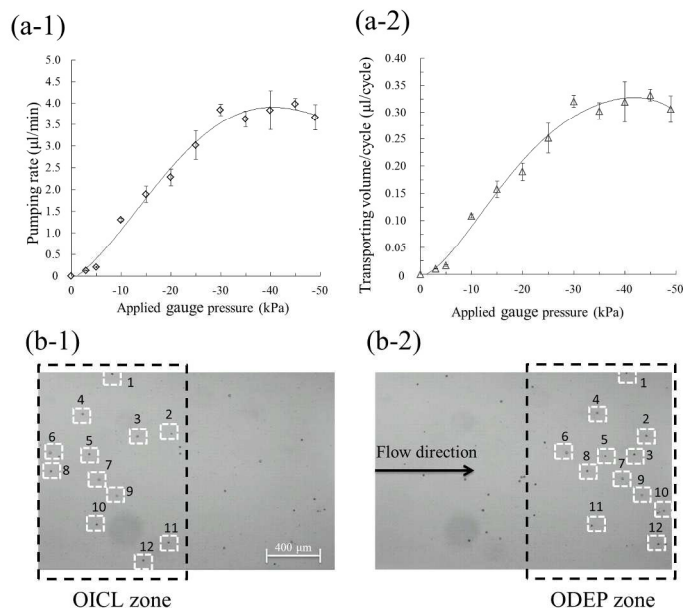
Characterization of the suction-type micropump for cell transporting and focusing

To automatically control the delivery of a group of cells from the inlet chamber to the outlet chambers, a suction-type micropump was used in this study. Such a pump can prevent the formation of dead volume, and the bubble formation in the microchannel [21]. Furthermore, the suction-type micropump avoids cell disruption as a result of deflection of the PDMS membrane when driven by high pressure. More importantly, it can control the membrane deflection at any particular time to transport very small ($\sim 0.045 \mu\text{l}$) sample volumes.

In order to automatically transport a group of cells for nucleus extraction, there is a need to sequentially complete the following steps: first, the cells must be injected into the inlet chamber. Secondly, a group of cells must be sucked into the suction-type micropump for transporting a pre-determined amount of sample. Third, a group of cells must be shuttled to the OICL zone for cell membrane lysis and consequent release of the nuclei. Finally the nucleus must be separated from the cell membrane debris in the ODEP zone. Initially, we calculated the minimum volume of sample in the OICL and the ODEP modules that the micropump transports HEK293T cells at one time. Figure 2(d) shows the dimensions of the OICL and ODEP zones in the microchannel formed by the double-sided tape (30- μm -thick). The volume of the OICL and ODEP zones was then calculated to be 0.045 μl (height \times width \times length = 0.03 mm \times 1.00 mm \times 1.50 mm).

After calculating the volume of the OICL and ODEP zones, we designed the suction-type micropump to serve as the flow control module. For successfully minimizing the transport rate of the micropump to be only 0.045 μl , we designed a PDMS cylinder plug (thickness = 300 μm , radius = 500 μm) in the middle of the microchannel (thickness = 550 μm , radius = 640 μm) to function as a stopper. Upon application of high pressure on the pneumatic layer, the maximum membrane deflection was limited to be only 250 μm and the transport rate could be limited to a small fixed volume. In Figure 4(a-1), the pumping rate of the suction-type micropump equipped with the PDMS plug has been demonstrated. The transported volume per cycle at which the micropump delivers one sample was also shown in Fig. 4(a-2). It was found that fine-tuning the pressure to -6.2 kPa resulted in the ability to transport a volume as small as 0.045 μl . Therefore, we successfully designed the suction-type micropump to transport a required small volume of cells into the OICL and ODEP zones to conduct cell membrane lysis and nucleus extraction, respectively (Fig. 4b).

Furthermore, the suction-type micropump that was designed and integrated into the flow control module could transport 0.2 M sucrose and HEK293T cells suspended in 0.2 M sucrose into the transport unit (micropump) such that all cells in 0.2 M sucrose were hydrodynamically focused into the downward channel (Fig. 4c). The results demonstrated that all of cells could be focused and ready to be lysed in the downward channel.



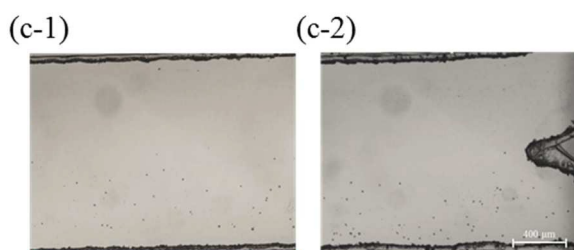


Figure 4: (a-1) The relationship between the pumping rate and the applied gauge pressure for the suction-type micropump ($n = 3$). (a-2) The relationship between the transported volume and the applied gauge pressure ($n = 3$). When the applied air gauge pressure was -6.2 kPa, the transported volume was $0.045 \mu\text{L}$ per cycle. (b) HEK293T cells were transported by the suction-type micropump from the OICL module to the ODEP module. (c) Picture of the cells guided and transported into the downward channel. After transporting by the suction-type micropump, HEK293T cells were guided in the front of microchannel (c-1) and at the back of the microchannel (c-2).

Cell membrane lysis without disruption of the nucleus by optically-induced electric fields

Optically-induced cell membrane lysis was realized by optimizing the voltage, driving frequency, light intensity, illumination time and radii of the light spots (not shown here). Such experiments involved the use of dually-stained cells that could be observed in real-time. First, different illumination time for single spots in a static flow was tested, as shown in Fig 5. The green and red fluorescence can be clearly seen for a period of 0.5 s (Figs. 5(b-1) to 5(b-4)), indicating that cells were intact. When cells were exposed to the OICL for 1.5 s, both green and red fluorescence vanished, indicating that complete cell lysis (membrane and nucleus) occurred (Figs. 5(d-1) to 5(d-4)). However, when the exposure time was adjusted to 0.9 s, only green fluorescence was observed, whereas the red fluorescence was not (Figs. 5(c-1) to 5(c-4)), indicating that cell membrane was successfully disrupted while the nucleus remained intact. These results show that one can selectively lyse cell membranes by adjusting the illumination time. Note that the applied AC voltage had been optimized to be 24 volts at a frequency of 8.5 kHz. The OICL light irradiance was set to be 3.2 W/cm^2 in this study. The projected pattern was a single spot with a diameter of $80 \mu\text{m}$; Note that, under these conditions, cells typically were lysed within 0.9 s in a static flow. Note that different illumination time for OICL operation may cause different situations. For the illumination time less than 0.9 s, the cells were observed to be only expanded. When cells were exposed to the applied electric field for more than 0.9 s, both nucleus and cell membrane were disrupted. Alternatively, when the exposure time was adjusted to be 0.9 s, nucleus was observed to remain intact whereas cell membrane was disrupted.

To further improve the throughput of nucleus extraction, we designed a multi-spot lighting system (diameter = $80 \mu\text{m}/\text{spot}$, see Fig. 2(d)) such that multiple cells could be lysed simultaneously. We applied this light spot array as virtual electrodes to induce cell membrane lysis, and most of the red fluorescence emerging from the cell membranes vanished after OICL, indicating successful membrane lysis. Note that the cell lysis in our device was only induced by OICL, which was dependent on applied voltage, frequency, illumination power intensity and illumination time. Detail information about the electric potential, electric field and transmembrane potential distribution could be found in Supplemental Information. Furthermore, the temperature increase

during the entire OICL and ODEP operation was measured to be within 2 degrees, which is much lower than the required temperature for thermal lysis.

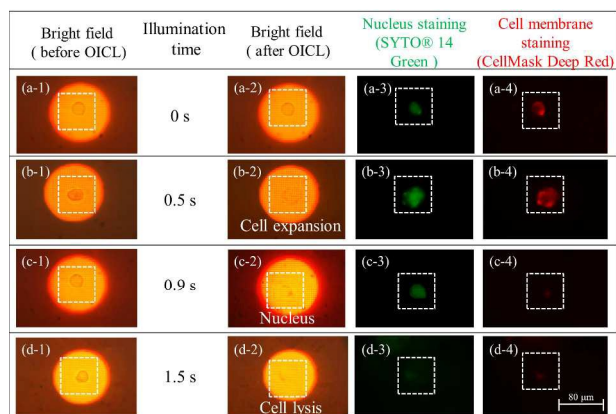


Figure 5: A series of images showing the relationship between cell membrane lysis and illumination time. (a-1) to (a-4): A series of cells before OICL. (b-1) to (b-4): Cell expansion after illumination for 0.5 s. (c-1) to (c-4): A series of photographs demonstrating that only cell membrane lysis took place after illumination for 0.9 s. (d-1) to (d-2): When the illumination time was increased to 1.5 s, both the nuclei and cell membranes were lysed.

Nucleus separation by ODEP

The maximum ODEP force and the maximum dragging velocity of cells were measured to be 7.55 pN and $28.30 \mu\text{m}/\text{sec}$, respectively. The displacement of the ODEP-driven separation was about $1528 \mu\text{m}$, and the ODEP separation process required 54 seconds at a maximum dragging velocity of $28.30 \mu\text{m}/\text{s}$. Compared with our previous work [28], our maximum dragging velocity was relatively weaker in our system. However, it still could be used for efficient separation of released nuclei and cell membrane debris. Note that the pumping rate was measured to be $0.27 \mu\text{L}/\text{min}$ during nucleus extraction experiments.

In the ODEP module, three moving-bars light patterns were used to separate nuclei and cell debris. Again, HEK293T cells were stained with green and red fluorescent dyes for the nucleus and cell membrane, respectively. Cells were first transported and focused in the microchannel with the flow control module. Before turning on the OICL and the ODEP module (Figures 6 (a)-6(c)), cells were guided to the downward channel, as expected. Then, after turning on the OICL and ODEP modules, the nuclei were then attracted from the downward to the upward channel by an ODEP force (Figures 6(d-f) while the cell membrane debris still stayed in the downward channel.

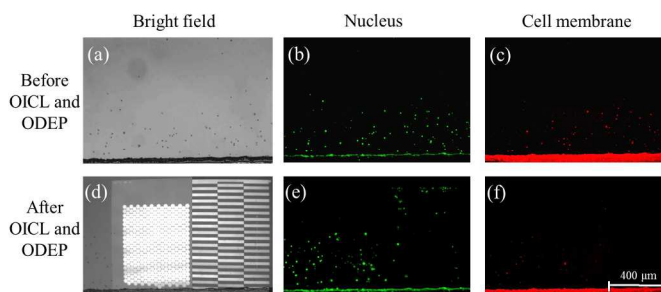


Figure 6: Images of the OICL and ODEP modules. (a) - (c): Cells in the microchannel before turning on the OICL and ODEP modules. (d) - (f): Cells in the microchannel after turning on the OICL and ODEP modules.

Efficiency of nucleus extraction

To calculate the nucleus extraction rate, samples were collected from the nucleus extraction chamber and the cell debris collection chamber (Fig. 7). Before OICL and ODEP (Figs. 7(a)-7(c)), the nucleus extraction chamber did not yield any green or red fluorescence, indicating that all cells were collected in another chamber (cell debris collection chamber). After OICL and ODEP (Figs. 7(d)-7(f)), it was observed that many nuclei only displaying green (and not red) fluorescence could be separated into the nucleus extraction chamber. It was then concluded that the collected samples in the nucleus extraction chamber were cell nuclei because the cell membranes had been disrupted (as evidenced by lack of red fluorescence).

After observing the nuclei isolated from the nucleus extraction chamber, fluorescent observation of the cell debris collection chamber was performed to serve as an additional quality control step (Figure 8). As expected, all cells were focused into the cell debris collection chamber due to the hydrodynamic focusing by 0.2 M sucrose (Figs. 8(a)-8(c)) before OICL and ODEP. After ODEP separation, most nuclei were separated to nucleus collection chamber such that the number of the nuclei in the cell debris collection chamber decreased significantly.

The cell membrane lysis rate and nucleus separation rate were then measured to be $78.04 \pm 5.70\%$ ($n=3$) and $80.90 \pm 5.98\%$ ($n=3$), respectively, which are comparable to values documented in previous works [25, 26]. Furthermore, the overall nucleus extraction rate was calculated to be 58.21% with a standard deviation of 2.21% in our integrated microfluidic system. Note that the cell counts were shown in the Supplemental information Table S1.

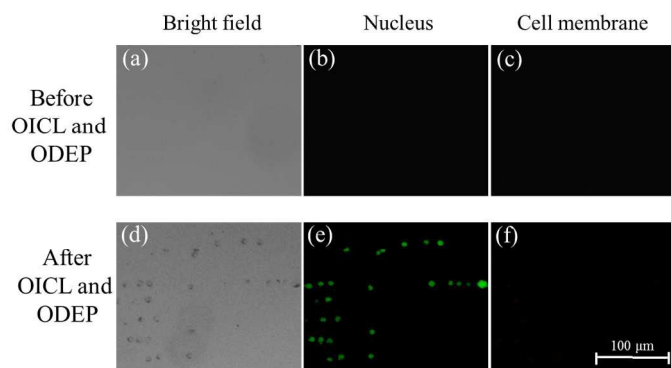
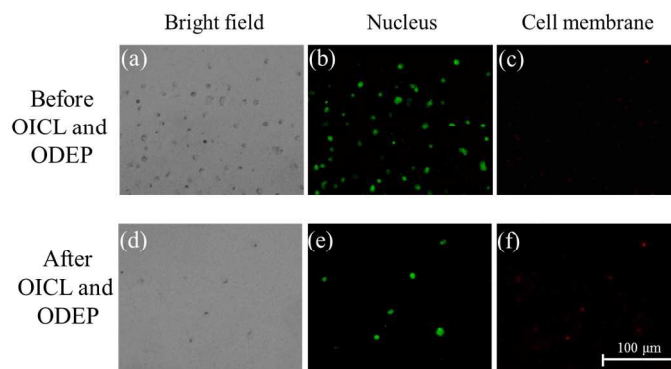


Figure 7: Nuclei and cell membrane debris in the nucleus extraction chamber before (a-c) and after (d-f) nuclear extraction.



8 | Lab on a chip

Figure 8: Nuclei and cell membrane debris in the cell debris collection chamber before (a-c) and after (d-f) nucleus extraction.

Conclusions

We have presented herein a new, integrated, OICL/ODEP microfluidic device for extraction of cell nuclei in a continuous-flow platform. Specifically, we successfully integrated a flow control module for transporting samples as small as 0.045 μl . In addition, the microchip contained two inlet chambers for injecting 0.2 M sucrose and HEK293T cells. When air pressure was applied, the 0.2 M sucrose aided in hydrodynamically focusing the cells. We finely tuned the operating conditions of the OICL to explore the optimal conditions for lysing cell membranes only without disrupting nuclei. We further integrated an ODEP module into our system and demonstrated that the nucleus could be readily separated from cellular debris. It is the first time that an integrated microfluidic chip was reported to feature both OICL and ODEP modules. The rates of cell membrane lysis, nucleus separation, and overall nucleus extraction were measured to be $78.04 \pm 5.70\%$, $80.90 \pm 5.98\%$, and $58.21 \pm 2.21\%$, respectively.

Our system has many advantages with respect to the traditional methods used for nucleus extraction. Firstly, the OICL/ODEP chip provided manoeuvrable virtual electrodes for selective lysis of the cell membrane followed by nuclear separation. It was particularly convenient due to the ease of manipulating the area upon which the optically-induced electrical field acted. Furthermore, we developed a flow control module and integrated it with the OICL/ODEP device to improve the throughput (= 80-120 cells/cycles, 1 cycle = 80 seconds) and enhance the nucleus extraction rate. Finally, cell focusing, cell transport, cell membrane lysis, and nucleus collection were all carried out on a single chip in a sequential and automated manner and did not require professional training to execute. By lysing cell membranes and releasing nuclei from a group of cells in a sequential fashion, high-throughput nuclear extraction could be achieved for a variety of biological applications.

Acknowledgements

The authors would like to thank financial support from Ministry of Science and Technology in Taiwan (MOST 104-2119-E-007-009). Partial financial support from the "Towards A World-class University Project" is also greatly appreciated.

Notes

^aDepartment of Power Mechanical Engineering, National Tsing Hua University, Hsinchu 30013, Taiwan; ^bInstitute of Biomedical Engineering, National Tsing Hua University, Hsinchu 30013, Taiwan; ^cInstitute of NanoEngineering and Microsystems, National Tsing Hua University, Hsinchu 30013, Taiwan

Corresponding author: *Dr. Gwo-Bin Lee; Department of Power Mechanical Engineering, National Tsing Hua University, Hsinchu 30013, Taiwan/ Fax: +886-3-5742495; Tel: +886-3-5715131 Ext. 33765; e-mail: gwobin@pme.nthu.edu.tw.

[†]Preliminary results in this manuscript were presented at the 9th IEEE International Conference on Nano/Micro Engineered and

Molecular Systems (IEEE NEMS 2014 Conference, Hawaii, USA, April 13-16, 2014) [29].

References

1. L. Nan, Z. Jiang and X. Wei, "Emerging microfluidic devices for cell lysis: a review," *Lab on a Chip*, 2014, 14(6): pp. 1060-1073.
2. T. Liehr, C. Uwe and G. Erich, "Nucleus extraction from single mounted tissue sections," *Genetic Analysis*, 1999, 15(2): pp. 65-69.
3. X. Chen, D. Cui, H. Cai, H. Li, J. Sun and L. Zhang, "MEMS-based microdevice for cell lysis and DNA extraction," *Microelectromechanical Systems and Devices*, 2012, pp. 23-39.
4. J. Fulka, P. Loi, H. Fulka, G. Ptak, T. Nagai, "Nucleus transfer in mammals: noninvasive approaches for the preparation of cytoplasts," *Trends in Biotechnology*, 2004, 22(6): pp. 279-283.
5. L. Chen, N. Patrone and J. F. Liang, "Peptide self-assembly on cell membranes to induce cell lysis," *Biomacromolecules*, 2012, 13(10): pp. 3327-3333.
6. L. A. Marshall, L. L. Wu, S. Babikian, M. Bachman and J. G. Santiago, "Integrated printed circuit board device for cell lysis and nucleic acid extraction," *Analytical Chemistry*, 2012, 84(21): pp. 9640-9645.
7. R.Z. Zare and S. Kim, "Microfluidic platforms for single-cell analysis," *Annual Review of Biomedical Engineering*, 2010, 12: pp. 187-201.
8. Y. H. Lin and G. B. Lee, "An integrated cell counting and continuous cell lysis device using an optically induced electric field," *Sensors and Actuators B: Chemical*, 2010, 145(2): pp. 854-860.
9. H. Lu, M. A. Schmidt and K. F. Jensen, "A microfluidic electroporation device for cell lysis," *Lab on a Chip*, 2004, 5(1): pp. 23-29.
10. X. Chen, D. Cui, H. Cai, H. Li, J. Sun and L. Zhang, "MEMS-based microdevice for cell lysis and DNA extraction," *Microelectromechanical Systems and Devices*, 2012, pp. 23-39.
11. J. Kim, M. Johnson, P. Hill and B. K. Gale, "Microfluidic sample preparation: cell lysis and nucleic acid purification," *Integrative Biology*, 2009, 1(10): pp. 574-586.
12. R. Brown, and J. Audet, "Current techniques for single-cell lysis," *Journal of the Royal Society Interface*, 2008, 5(2): pp. 131-138.
13. C. Witte, C. Kremer, J. M. Cooper and S. L. Neale, "Continuous cell lysis in microfluidics through acoustic and optoelectronic tweezers," *Proceedings of SPIE*, 2014, doi: 10.1117/12.2004814.
14. M. Hagiwara, T. Kawahara, L. Feng, Y. Yamanishi and F. Arai, "On-chip dual-arm microrobot driven by permanent magnets for high speed cell enucleation," *Journal of Micro Electro Mechanical Systems*, 2011, pp. 189-192.
15. F. Arai, N. Inomata, S. Kudo, Y. Yamanishi, T. Mizunuma, "Omni-directional actuation of magnetically driven microtool for enucleation of oocyte," *Journal of Micro Electro Mechanical Systems*, 2010, pp. 1167
16. Q. Zhao, M. Cui, C. Zhang, J. Yu, M. Sun and X. Zhao, "Robotic enucleation for oocytes," *Proceedings of IEEE Nano/Micro Engineered and Molecular Systems (NEMS)*, 2014, pp. 23-27.
17. Y. H. Lin and G. B. Lee, "An optically induced cell lysis device using dielectrophoresis," *Applied Physics Letters*, 2009, pp. 033901.
18. P. Y. Chiou, A. T. Ohta and M. C. Wu "Massively parallel manipulation of single cells and microparticles using optical images," *Nature*, 2005, 436(7049): pp. 370-372.
19. W. Y. Lin, Y. H. Lin and G. B. Lee, "Separation of microparticles utilizing spatial difference of optically induced dielectrophoretic forces," *Microfluidics and Nanofluidics*, 2009, 8(2): pp. 217-229.
20. A. Ashkin, J. M. Dziedzic, J. E. Bjorkholm and S. Chu, "Observation of a single-beam gradient force optical trap for dielectric particles," *Optics Letters*, 1986, 11(5): pp. 288-290.
21. C. H. Weng, K.Y. Lien, S. Y. Yang, G. B. Lee, "A suction-type, pneumatic microfluidic device for liquid transport and mixing," *Microfluidics and Nanofluidics*, 2011, 10(2): pp. 301-310.
22. W. H. Chang, C. H. Wang, S. Y. Yang, Y. C. Lin, J. J. Wu, Mel S. Lee and G. B. Lee, "Rapid isolation and diagnosis of live bacteria from human joint fluids by using an integrated microfluidic system," *Lab on a Chip*, 2014, 14(17): pp. 3376-3384.
23. H. Y. Hsu, A. T. Ohta, P. Y. Chiou, A. Jamshidi, S. L. Neale and M. C. Wu, "Phototransistor-based optoelectronic tweezers for dynamic cell manipulation in cell culture media," *Lab on a Chip*, 2010, 10(2): pp. 165-172.
24. W. Choi, S. H. Kim, J. Jang and J. K. Park, "Lab-on-a-display: a new microparticle manipulation platform using a liquid crystal display (LCD)," *Microfluidics and Nanofluidics*, 2007, 3(2): pp. 217-225.
25. X. B. Wang, Y. Huang, F. F. Becker and P. R. C. Gascoyne, "A unified theory of dielectrophoresis and travelling wave dielectrophoresis," *Journal of Physics D: Applied Physics*, 1994, 27(7): pp. 1571-1574.
26. R. G. Panchal, K. P. Kota, K. B. Spurgers, G. Ruthel, J. P. Tran, R. C. "Dutch" Boltz and S. Bavari, "Development of high-content imaging assays for lethal viral pathogens," *Journal of Biomolecular Screening*, 2010, 15(7): pp. 755-765.
27. R. B. Knowles, J. H. Sabry, M. E. Martone, T. J. Deerinck, M. H. Ellisman, G. J. Bassell and K. S. Kosik, "Translocation of rna granules in living neurons," *Journal of Neuroscience*, 1996, 16(24): pp. 7812-7820.
28. S. B. Huang, M. H. Wu, C. H. Hsieh, H. C. Lin, C. P. Tseng and G. B. Lee, "High-purity and label-free isolation of circulating tumor cells (CTCs) in a microfluidic

- platform by using optically-induced- dielectrophoretic (ODEP) force,” *Lab on a Chip*, 2013, 13(7): p. 137-183.
29. S. S. Huang, L. Y. Hung, and G. B. Lee, “Nucleus extraction from cells by optical-induced cell lysis on a continuous flow platform,” *Proceedings of IEEE Nano/Micro Engineered and Molecular Systems (NEMS)*, 2014, pp. 436-439.